IMPACT OF HEAT TRANSFER ANALYSIS ON CARREAU FLUID FLOW PAST A STATIC/MOVING WEDGE

by

HASHIM Ali and *Masood KHAN*

Department of Mathematics, Quaid-i-Azam University 45320, Islamabad 44000 , Pakistan

Abstract

The foremost aspiration of the present endeavor is to investigate the boundary layer flow of a generalized Newtonian Carreau fluid model past a static/moving wedge. In addition, the effects of heat transfer on the flow field are also taken into account. The governing equations of the problem based on the boundary layer approximation are changed into a non-dimensional structure by introducing the local similarity transformations. The subsequent system of ordinary differential equations has been numerically integrated with fifth-order Runge-Kutta method. Influence of the velocity ratio parameter λ, the wedge angle parameter β, the Weissenberg number We, the power law index n and the Prandtl number Pr on the skin friction and Nusselt number are analyzed. The variation of the skin friction as well as other flow characteristics has been presented graphically to capture the influence of these parameters. The results indicate that the increasing value of the wedge angle substantially accelerates the fluid velocity while an opposite behavior is noticed in the temperature field. Moreover, the skin friction coefficient for the growing Weissenberg number significantly enhances for the shear thickening fluid and show the opposite behavior of shear thinning fluid. However, the local Nusselt number has greater values in the case of moving wedge. An excellent comparison with previously published works in various special cases has been made.

Keywords: Carreau fluid model; Boundary layer flow; Heat transfer analysis; Static/Moving wedge; Runge-Kutta method.

Introduction

During the last few decades, the fluid flows across wedge shaped bodies are of fundamental importance in numerous engineering applications. It has a broad occurance in the fields of aerodynamics, heat exchangers, hydrodynamics, geothermal systems, etc. Specifically, such sort of flow happens as often as possible in enhanced oil recovery, aircraft response to atmospheric gusts, packed bed reactor geothermal industries, ground water pollution and so forth. Historically, Falkner and Skan [1] concentrated the flow over a static wedge in early 1930, which is immersed in a viscous fluid and introduced the Falkner-Skan equation. In this study, they outlined the Prandtl's boundary layer hypothesis and utilized the similarity transformations to diminish the overseeing boundary layer equations to ordinary differential equations. In the previous couple of years, analysts have demonstrated extraordinary enthusiasm for the Falkner-Skan flow by considering the impacts of various parameters. The solutions and their reliance on β (the wedge angle) were likewise later inspected by Hartree [2]. He acquired the solutions as far as velocity distribution for different estimations of pressure gradient parameters. In the meantime, an all the more fascinating problem in this regard was considered by Riley and Weidman [3]. They focused on the impacts of moving boundary on a wedge in a viscous fluid and applied a similarity variable which prompted a nonlinear third-order ordinary differential equation and settled it numerically. Additionally, Watanabe [4] investigated the behavior of boundary layer forced flow over a wedge with uniform suction or injection. As of late, Ishak *et al.* [5] examined the magnetohydrodynamic flow of a conducting fluid streaming transversely with variable magnetic field along a moving wedge.

The boundary layer theory is to a great degree prospering admiration in the historical backdrop of Newtonian fluid mechanics (see Schlichting and Gersten [6]). A few fluid flow problems and their heat exchange attributes have been effectively displayed with the aid of this theory and the results agree very well with experimental observations. Some late learns about the boundary layer flow of Newtonian fluids are given in [7 – 10]. Nonetheless, numerous mechanical fluids are non-Newtonian in their flow characteristics and are alluded to as rheological fluid models. It is currently a perceived reality that non-Newtonian fluids have a larger number of utilization in engineering than Newtonian fluids. Such examples incorporates into pharmaceuticals, fiber innovation, products of everyday sustenance, crystal growth, and so on. One specific class of such materials which is of noteworthy interest is that in which the effective viscosity relies on upon the rate of shearing. Such fluids are termed as generalized Newtonian fluids (GNF). The rheological equations of GNF have been cultivated from the Newtonian constitutive relations to suspect the deformation stresses in a non-Newtonian fluid. The constitutive equation for the generalized Newtonian fluids can be expressed as follows:

$$\tau = \mu(\dot{\gamma})\boldsymbol{A_1}, \tag{1}$$

where $\mu(\dot{\gamma})$ is titled as the generalized Newtonian viscosity, τ represents the stress tensor and $\boldsymbol{A_1}$ is termed as the rate of strain tensor. The function $\mu(\dot{\gamma})$ is to be specified and it has different expressions for various fluid models, such as power-law, Sisko and Carreau models (see Bird *et al.* [11] and Slattery [12]). The rheological equation for the Carreau model [13] is a particular example of the GNF in which the apparent viscosity μ changes with the magnitude $\dot{\gamma}$ of the deformation rate. The Carreau rheological model appropriately portrays the non-Newtonian conduct of numerous lubricants [14, 15]. This rheological model has a hypothetical premise [13] and imitates the viscosity of a few real fluids, like polymer solutions, over a very extensive range for the values of $\dot{\gamma}$, as appeared for occurrence in [11]. The governing relationship for apparent viscosity $\mu(\dot{\gamma})$ that will be considered here is [13]:

$$\mu = \mu_\infty + (\mu_0 - \mu_\infty)[1 + (\Gamma\dot{\gamma})^2]^{\frac{n-1}{2}}. \tag{2}$$

The two material parameters Γ and n appearing in the Carreau model depict the shear rate reliance of the viscosity. Here μ_0 represents the zero shear viscosity and μ_∞ the infinite shear viscosity. The power law index n controls the slope of $(\mu - \mu_\infty)/(\mu_0 - \mu_\infty)$ in the power law region. The fluid is characterized as shear thinning for $0 < n < 1$ shear thickening for $n > 1$ and Newtonian for $n = 1$. As the shear rate becomes larger the Carreau model behaves as power-law fluid and at low shear rate it behaves as Newtonian fluid. In current formulation, we considered here a vanishing viscosity at an infinite rate of strain i.e. $\mu_\infty = 0$. A very few studies are concerned with the Carreau fluid flowed their and heat transfer characteristics in the past few years. For instance, Khellaf and Lauriat [16] investigated the flow and heat transfer in a short vertical annulus with a heated and rotating inner cylinder. Olajuwon [17] studied the convection heat and mass transfer of MHD Carreau fluid past a vertical porous plate. Also, numerical investigation of inertia and shear thinning effects on axisymmetric flows of Carreau fluids was reported by Martins *et al.* [18]. Recently, the boundary layer flow and heat transfer to a Carreau fluid over a non-linear stretching sheet is discussed by Khan and Hashim [19].

This article addresses the impacts of the heat transfer analysis on the flow of GN Carreau fluid over a static/moving wedge. New outgrowths are given in this investigation to manifest the occurrence of the locally similar solutions. Scaling group of transformations is utilized to present the local similarity representations of the governing partial differential equations. An efficient fifth-order Runge–Kutta scheme is used to solve the similarity equations. The impacts of the relevant flow variables are depicted in point of interest through graphs and tables. To the best of the author's information, there is no endeavor highlighting the above expressed flow model for Carreau fluid.

Basic equations

We consider the laminar, incompressible and two-dimensional flow of a GN Carreau fluid over a static/ moving wedge. It is assumed that the wedge is moving with the velocity $u_w(x) = bx^m$ and the velocity of the free stream is $u_e(x) = cx^m$, where b, c and m are constants. We use the rectangular coordinates (x, y), in which x and y are the distances measured along the wedge and normal to surface of the wedge. Further, the origin of the Cartesian coordinates (x, y) is at the tip of the wedge. The physical configuration and coordinate systems appear in figure 1. Here $u_w(x) > 0$ compares to a stretching wedge surface velocity and $u_w(x) < 0$ relates to a contracting wedge surface velocity. The temperature at sheet T_w is assumed to be constant and the ambient temperature is T_∞, where $T_\infty < T_w$.

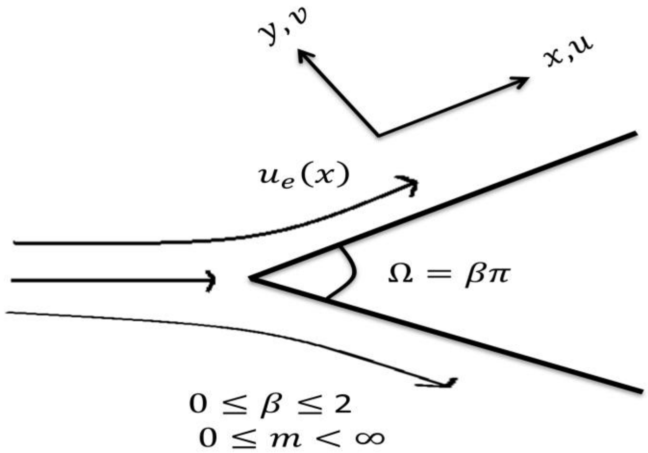

Figure 1: Schematic of physical model.

Under the boundary layer approximations, we have the following governing equations.
Conservation of mass:

$$\frac{\partial u}{\partial x} + \frac{\partial v}{\partial y} = 0, \tag{3}$$

Conservation of momentum [13]:

$$u\frac{\partial u}{\partial x} + v\frac{\partial u}{\partial y} = u_e\frac{du_e}{dx} + \nu\frac{\partial^2 u}{\partial y^2}\left[1+\Gamma^2\left(\frac{\partial u}{\partial y}\right)^2\right]^{\frac{n-1}{2}} + \nu(n-1)\Gamma^2\frac{\partial^2 u}{\partial y^2}\left(\frac{\partial u}{\partial y}\right)^2\left[1+\Gamma^2\left(\frac{\partial u}{\partial y}\right)^2\right]^{\frac{n-3}{2}}, \tag{4}$$

Conservation of energy:

$$u\frac{\partial T}{\partial x} + v\frac{\partial T}{\partial y} = \alpha\frac{\partial^2 T}{\partial y^2}, \tag{5}$$

in which (u, v) are the velocity components in (x, y), directions, respectively, ν be the kinematic viscosity, Γ a material parameter often referred as relaxation time, α the thermal diffusivity of the fluid, T the temperature of the fluid and n being the power-law index.
The relevant boundary conditions are

(1) static wedge

$$u = 0, \quad v = 0, \quad T = T_w, \quad \text{at} \quad y = 0, \tag{6}$$

$$u = u_e(x) = cx^m, \quad T \to T_\infty, \quad \text{as} \quad y \to \infty. \tag{7}$$

(2) moving wedge

$$u = u_w(x) = bx^m, \ v = 0, \ T = T_w, \quad \text{at} \quad y = 0, \tag{8}$$

$$u = u_e(x) = cx^m, \quad T \to T_\infty, \quad \text{as} \quad y \to \infty. \tag{9}$$

To look at the flow regime, we present the accompanying locally similar transformations:

$$\psi(x,y)=\sqrt{\frac{2\nu c}{m+1}}x^{\frac{m+1}{2}}f(\eta) \qquad \eta=y\sqrt{\frac{c(m+1)}{2\nu}}x^{\frac{m-1}{2}}, \qquad \theta(\eta)=\frac{T-T_\infty}{T_w-T_\infty}, \tag{10}$$

where ψ is the stream function, characterized in the standard way as $u=\frac{\partial\psi}{\partial y}$ and $v=-\frac{\partial\psi}{\partial x}$. Thus, the velocity components using the above similarity transformation are given as:

$$u=cx^m f'(\eta), \quad v=-\sqrt{\frac{b(m+1)\nu}{2}}x^{\frac{m-1}{2}}\left\{f(\eta)+\eta\left(\frac{m-1}{m+1}\right)f'(\eta)\right\} \tag{11}$$

By employing Eqs. (10) and (11), the momentum and energy Eqs. (4) and (5) takes the form:

$$\left\{1+nWe^2\left(f''\right)^2\right\}\left\{1+We^2\left(f''\right)^2\right\}^{\frac{n-3}{2}}f'''+ff''+\beta\left(1-\left(f'\right)^2\right)=0, \tag{12}$$

$$\theta''+\Pr f\theta'=0. \tag{13}$$

The changed boundary conditions are as per the following:

$$f(0)=0, \quad f'(0)=\lambda, \quad \theta(0)=1, \tag{14}$$

$$f'(\infty)\to 1, \qquad \theta(\infty)\to 0. \tag{15}$$

In the above expressions, primes mean differentiation with respect to η, β is the wedge angle parameter, λ the constant velocity ratio parameter, We the local Weissenberg number and $\Pr$ the Prandtl number. These parameters are defined as:

$$\beta=\frac{2m}{m+1}, \quad \lambda=\frac{b}{c}, \quad We=\left(\frac{c^3\Gamma^2x^{3m-1}}{2\nu}\right)^{1/2}, \quad \Pr=\frac{\mu c_p}{k}. \tag{16}$$

In accordance with [1], the included angle of the wedge is taken to be $\Omega=\beta\pi$, where $\beta=\frac{2m}{m+1}$ is known as the wedge angle parameter. Physically, the wedge angle parameter β is related to the pressure gradient in such a way that the positive values of β representing the favorable pressure gradient and negative values of β demonstrates an adverse pressure gradient. Further, $m=0$, *i.e.* $(\beta=0)$ means the fluid flow past a flat plate and $m=1$, *i.e.* $(\beta=1)$ implies the stagnation point flow. Additionally, the constant velocity ratio parameter $\lambda>0$ and $\lambda<0$ identifies with a moving wedge in the same and inverse directions to the free stream, separately, while $\lambda=0$ compared to a static wedge

Parameters of practical interest

We are interested in the skin friction coefficient C_f and the local Nusselt number Nu, individually. Physically, C_f is the shear stress at surface and Nu represents the rate of heat transfer at the wall. Conventionally, these are characterized as:

$$C_f=\frac{\tau_w}{\rho u_w^2/2}, \qquad Nu=\frac{xq_w}{k\left(T_w-T_\infty\right)}. \tag{17}$$

in which:

$$\tau_w=\mu_0\frac{\partial u}{\partial y}\left[1+\Gamma^2\left(\frac{\partial u}{\partial y}\right)^2\right]^{\frac{n-1}{2}}\Bigg|_{y=0}, \quad q_w=-k\left(\frac{\partial T}{\partial y}\right)\Bigg|_{y=0}. \tag{18}$$

Using the similarity variables $(10)-(11)$, we get the corresponding expressions:

$$\mathrm{Re}^{1/2}C_f = \frac{2}{\sqrt{2-\beta}} f''(0)\left[1+We^2\left(f''(0)\right)^2\right]^{\frac{n-1}{2}}, \quad \mathrm{Re}^{-1/2}Nu = -\frac{2}{\sqrt{2-\beta}}\theta'(0), \tag{19}$$

in which the local Reynolds number is defined as $\mathrm{Re}=\frac{xu_e}{\nu}$.

Numerical simulation

The system of differential equations $(12)-(15)$ is highly nonlinear and partially coupled so these equations cannot be solved analytically. For this purpose a numerical treatment would be much more suitable. Thus, the boundary value problems (12) and (13) with boundary conditions (14) and (15) have been numerically solved by applying fifth-order Runge-Kutta integration technique together with shooting iteration scheme in a computer software MATLAB. In order to apply the said technique, we need to rewrite the boundary value problems as systems of first-order ODEs. We have placed Eqs. (12) and (13) as first order differential equations by supposing $\left(f, f', f'', \theta, \theta'\right)=\left(U_1, U_2, U_3, U_4, U_5\right)=U$, as follows:

$$U_1' = U_2,\; U_2' = U_3,\; U_3' = \frac{-U_1U_3-\beta\left\{1-\left(U_2\right)^2\right\}}{\left\{1+nWe^2\left(U_3\right)^2\right\}\left\{1+We^2\left(U_3\right)^2\right\}^{\left(\frac{n-3}{2}\right)}},\; U_4' = U_5,\; U_5' = -\mathrm{Pr}\,U_1U_5. \tag{19}$$

The corresponding initial conditions become:

$$U^{\mathrm{T}} = \left(0, \quad \lambda, \quad U_3, \quad 1, \quad U_5\right) \tag{20}$$

The basic idea of shooting method is to calculate the unknown (unspecified) boundary conditions. We noticed that above system contains unknown values U_3 and U_5 *i.e.* $f''(0)$ and $\theta'(0)$ that needs to be determined by guessing in order to solve above system of Eq. (19) subject to initial conditions (20). To apply this method, the most important step is to pick some pertinent finite value of $\eta \to \infty$ namely $\eta=\eta_{max}$. In this way, the solutions were acquired by various initial speculations for the missing estimations of $f''(0)$ and $\theta'(0)$. The technique is to regard these terms as certain values that ought to be resolved ahead of time, and afterward an additional iterative loop in the program has been connected to locate these specific values in a way that fulfills the far field conditions, i.e. $f'(\eta_{\max})=1$ and $\theta(\eta_{max})=0$. After that integration is carried out and compare with the boundary conditions at $\eta=\infty$. In the present analysis, we have chosen a suitable finite value of $\eta\to\infty$, namely $\eta=\eta_{\max}$, between 5 and 10. A step size of $\Delta\eta=0.01$ was chosen to be acceptable for a convergence basis of 10^{-6} for all cases.

Testing of Code

In order to validate the current numerical scheme, we have computed the values of skin friction coefficient $Re^{1/2}C_f$ for distinct values of β with those results obtained by Rajagopal *et al.* [20], Kuo [21] and Ishak *et al.* [22] for Newtonian case. It is conspicuous from table 1, that the information delivered by the present code is in radiant concurrence with prior published results. Thus we are very sure that the present results are exact.

Table **1:** Numerical values of the skin friction coefficient $Re^{1/2}C_f$ for various β when $n = 1.0$ and $We = 0.0$ are fixed.

β	**Rajagopal *et al*.** [20]	**Kuo** [21]	**Ishak *et al.*** [22]	**Present study**
0.0		0.469600	0.4696	0.469601
0.1	0.587035	0.587880	0.5870	0.587036
0.3	0.774755	0.775524	0.7748	0.774754
0.5	0.927680	0.927905	0.9277	0.92768
1.0	1.232585	1.231289	1.2326	1.232587

Furthermore, to evaluate the exactness of the numerical technique, estimations of the local Nusselt number $Re^{-1/2}Nu$ are contrasted with already published work. Table 2 looks at the estimations of $-\theta'(0)$ for various Prandtl numbers in the limiting cases. We watched that the outcomes acquired in the present study are observed to be in brilliant concurrence with those got by before analysts.

Table **2:** Numerical values of the Nusselt number $Re^{-1/2}Nu$ for various values of Pr and β when $n = 1.0$ and $We = 0.0$ are fixed.

	$\beta = 0$		$\beta = 0.3$	
Pr	**White** [23]	**Present study**	**White** [23]	**Present study**
0.1	0.1980	0.198032	0.2090	0.209075
0.3	0.3037	0.303718	0.3278	0.327829
0.6	0.3916	0.391677	0.4289	0.428925
0.72	0.4178	0.418093	0.4592	0.459552
1.0	0.4696	0.469602	0.5195	0.519521
2.0	0.5972	0.597241	0.6690	0.669046
6.0	0.8672	0.867296	0.9872	0.987274
10.0	1.0297	1.029754	1.1791	1.179136

Results and discussion

Numerical simulation was performed to investigate the momentum and also the thermal boundary layer analysis for a two dimensional flow of GN Carreau fluid generated by a static/moving wedge. For this reason, the impact of non-dimensional overseeing parameters $n,\ We,\ \beta,\ \lambda$ and Pr on dimensionless fluid velocity and temperature profiles, alongside with the friction factor coefficient and local Nusselt numbers, are concentrated on and displayed through graphs. Henceforth, the numerical results are exhibited in two segments– fluid flow and heat transfer, respectively.

Computational results for fluid flow

Velocity profiles portrayed in figures $2(a)$ and $2\ (b)$ demonstrates the impact of velocity ratio parameter λ for both shear thinning and shear thickening regimes. All the model curves fulfill the far field boundary conditions (14) asymptotically, along these lines supporting the numerical calculations. It regards see that the velocity profiles are bestowed for two distinctive instances of β, specifically, $\beta = 0.0$ that relates to the wedge edge of zero degree, i.e. flow past a flat plate and $\beta = 1.0$ which compares to the wedge point of

90° i.e. a stagnation-point flow. From these trajectories, we perceived that the fluid velocity is accelerated by increasing values of the velocity ratio parameter for both cases. We notice from figure 2 that momentum boundary layer thickness is thinner in case of stagnation-point flow when contrasted with flow over a flat plate. From physical perspective, it is because of the way that the pressure force together with inertia force has a tendency to decrease the impact of viscous forces in the boundary layer. It can be further seen that in case of flow near the stagnation-point, the velocity curves are closer to each other. Additionally, these figures present that the thickness of the momentum boundary layer for shear thickening fluid is higher in comparison with shear thinning fluid.

Figures 3(a) and 3(b) illustrates the dimensionless fluid profiles inside the boundary layer for various estimations of the wedge angle parameter β if there should arise an occurrence of static or moving wedge. For each situation, a considerable increment in the velocity profile is sighted for more grounded estimations of β. From a physical perspective, the wedge angle parameter β represent the pressure gradient, so the positive values of β mean a favorable pressure gradient which accelerates the flow. It is important to mark that if there should arise an occurrence of accelerated flows, i.e. positive estimations of β, the velocity curves crush closer and nearer to the surface of the wedge, and reverse flow does not happen. Further, the momentum boundary layer thickness diminishes by expanding β and then again it is higher if there should be an occurrence of shear thickening fluid.

The impacts of the velocity ratio parameter λ, the wedge angle parameter β and power law index n on the local skin friction coefficient $Re^{1/2}C_f$ are portrayed in figures 4 and 5. It is shown in figure 4 that the velocity ratio parameter λ has a great effect on the skin friction coefficient in both shear thinning and thickening cases. Besides, a watchful inspection of figure 4 reveals that the local skin friction of Carreau fluid can be reduced by enlarging the values of λ. On the other hand, we noticed that with rising values of the Weissenberg number We, the skin friction increases for shear thickening fluids while an opposite is true in case of shear thinning fluids. In addition, figure 5 indicates the dependency of local skin friction $Re^{1/2}C_f$ on the wedge angle parameter β. Concerning the friction coefficient, a monotonic growth is found with an expansion in the values of β. Also, the local skin friction is lessor in case of a moving wedge in comparison with in the case of static wedge.

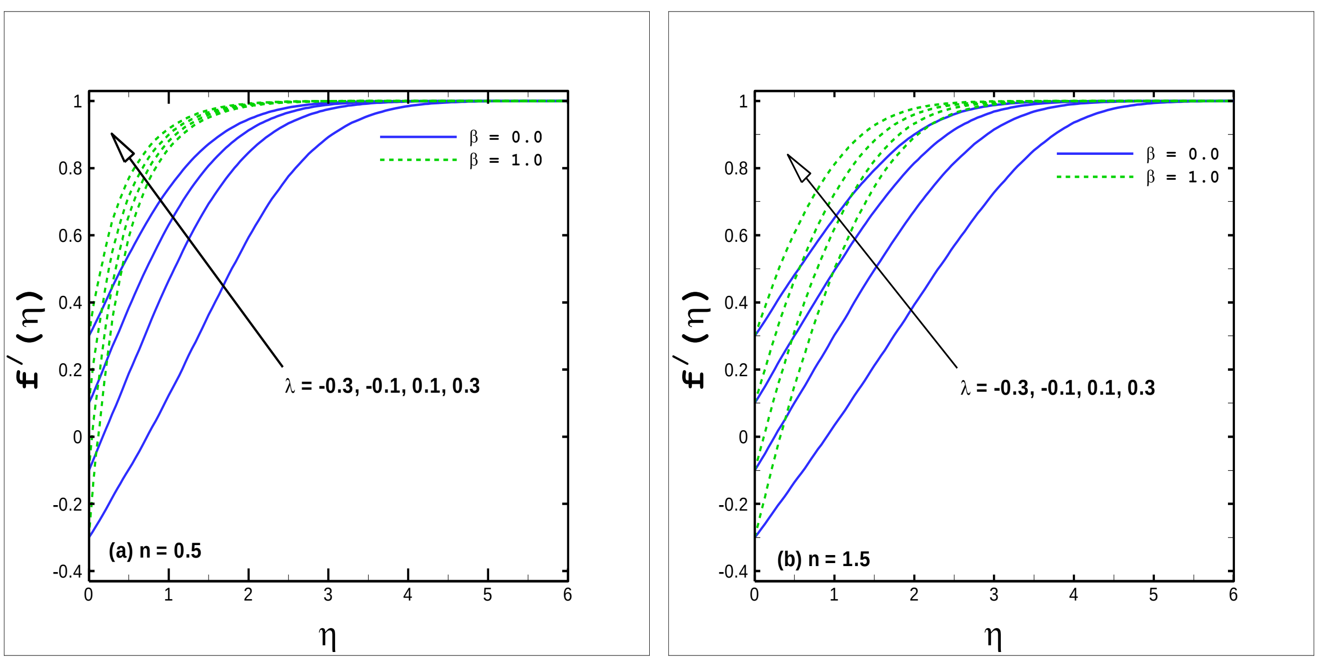

Figure 2: Velocity profiles $f'(\eta)$ for different λ with $We = 3.0$.

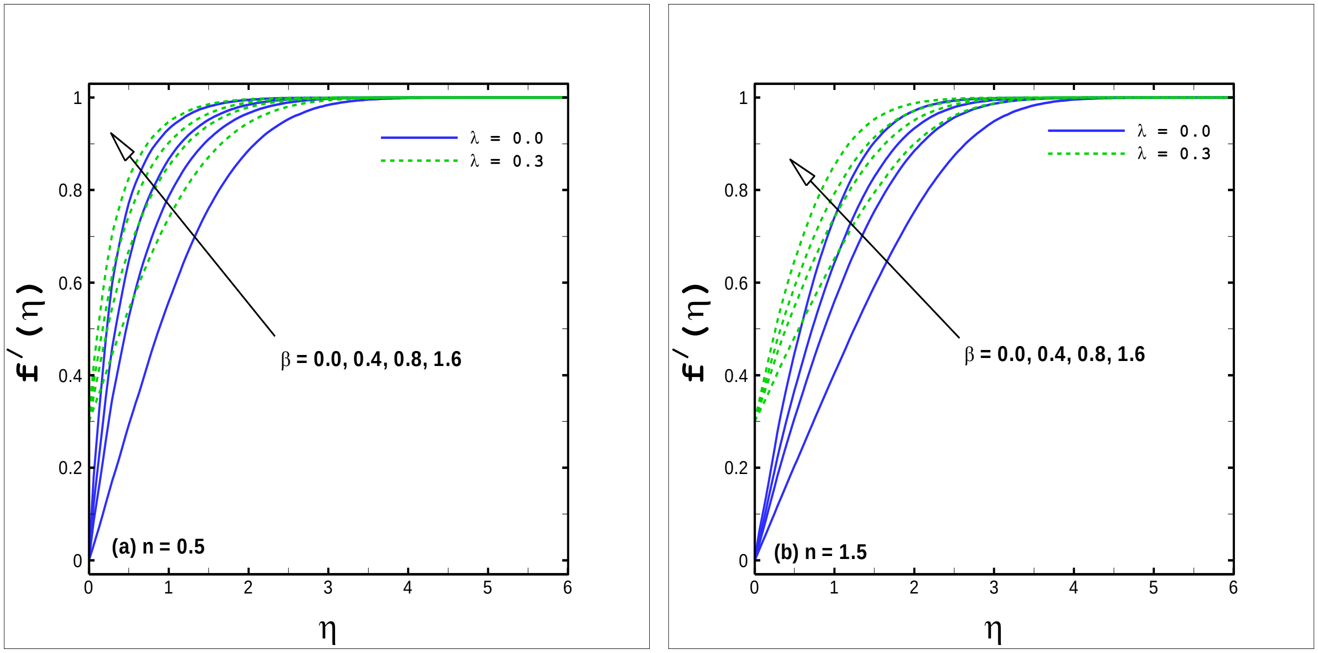

Figure 3: Velocity profiles $f'(\eta)$ for different β with $We = 3.0$.

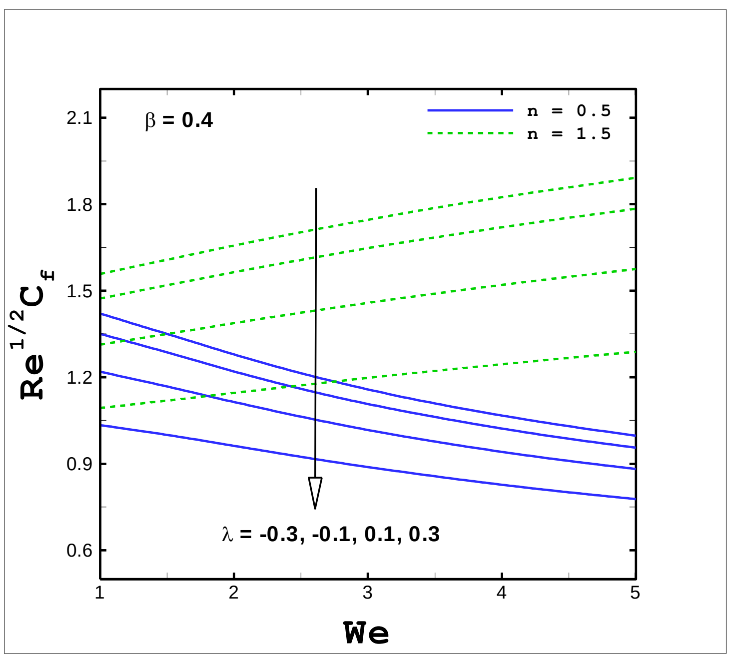

Figure 4: Variation of the skin friction coefficient $Re^{1/2}C_f$ with We for different λ.

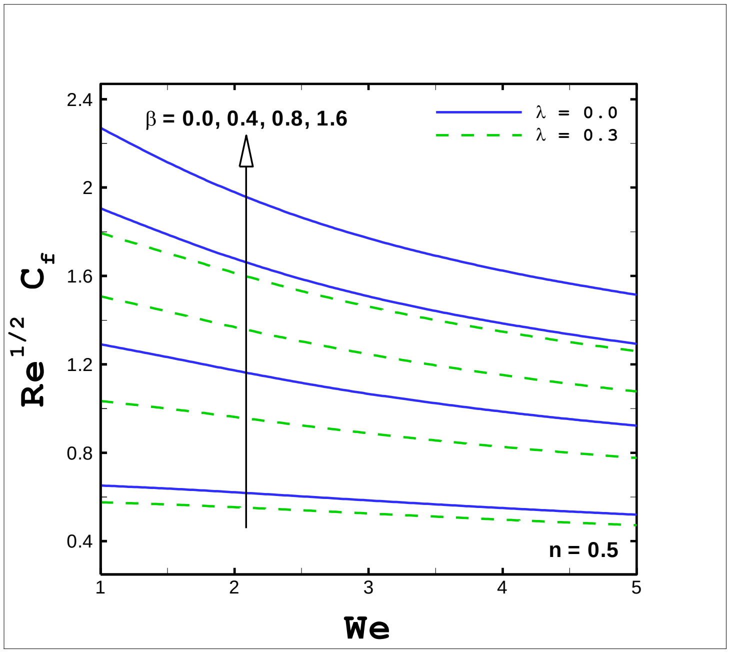

Figure 5: Variation of the skin friction coefficient $Re^{1/2}C_f$ with We for different β.

Computational results for heat transfer

Some physical bits of knowledge into the way of heat exchange can be picked up by analyzing the non-dimensional temperature profiles and local Nusselt number variation from the surface of the wedge.

Figure 6 is a plot of the variation in the non-dimensional temperature $\theta(\eta)$ within the boundary layer for distinct values of the velocity ratio parameter λ. These figures $6(a)$ and $6(b)$ reveal that the fluid temperature shows a decreasing behavior with the flourishing values of the velocity ratio parameter λ in both cases, i.e. for shear thinning as well as shear thickening fluids. The thermal boundary layer thickness decreases for both the flow over flat plate and near the stagnation-point. Anyhow, the temperature profiles merely nearer to each other if there should be an occurrence of flow near to the stagnation-point and the thickness of the thermal boundary layer is higher for shear thickening fluid.

Concerning the impact of wedge angle parameter β on thermal boundary layer, figures $7(a)$ and $7(b)$ manifests the temperature profiles for different values of $\beta = (0, 0.4, 0.8, 1.6)$. We observed that the fluid temperature is firmly depressed with increasing the wedge angle parameter. Moreover, the maximum temperature of the fluid can be accomplished for the flow over flat plate $\beta = 0$. Physically, this happens on the grounds that for $\beta = 0$, the driving force to the fluid motion (pressure gradient) is zero and as a result of that the fluid temperature at the surface of the wedge enhances. In the event of static wedge thickness of the thermal boundary layer is higher.

The variance in non-dimensional temperature for various estimations of the Weissenberg number We is lit up in figures $8(a)$ and $8(b)$. These figures delineate that the dimensionless temperature profiles are contracted for shear thinning fluid with an expansion in the Weissenberg number. Be that as it may, a remarkable inverse conduct is caught in the shear thickening fluid. The impacts of Prandtl number on the fluid temperature are to decelerate the temperature as appeared in figure 8. The Prandtl number is the proportion of momentum diffusivity to thermal diffusivity. At the point when $Pr = 1.0$, both momentum and thermal diffusivities are equivalent, however when $Pr > 1.0$, the momentum diffusivity is more prominent than thermal diffusivity and the thermal boundary layer thickness diminishes with the large Prandtl number. Likewise, the thermal boundary layer thickness is higher in shear thickening fluids.

At long last, the physical quantity, for example, the local Nusselt number $Re^{-1/2}Nu$ is plotted in figures 9 and 10 against the Weissenberg number We for different parameters like n, β and λ. The results for variation of the local Nusselt number with few estimations of the velocity ratio parameter λ are presented in figure 9. A substantial increase in the local Nusselt number is seen for the larger values of λ. However, an enhancement in the wedge angle parameter β accelerates the magnitude of the local Nusselt number as depicted in the figure 10. as expected the values of local Nusselt number show an increasing behavior by uplifting the Weissenberge number.

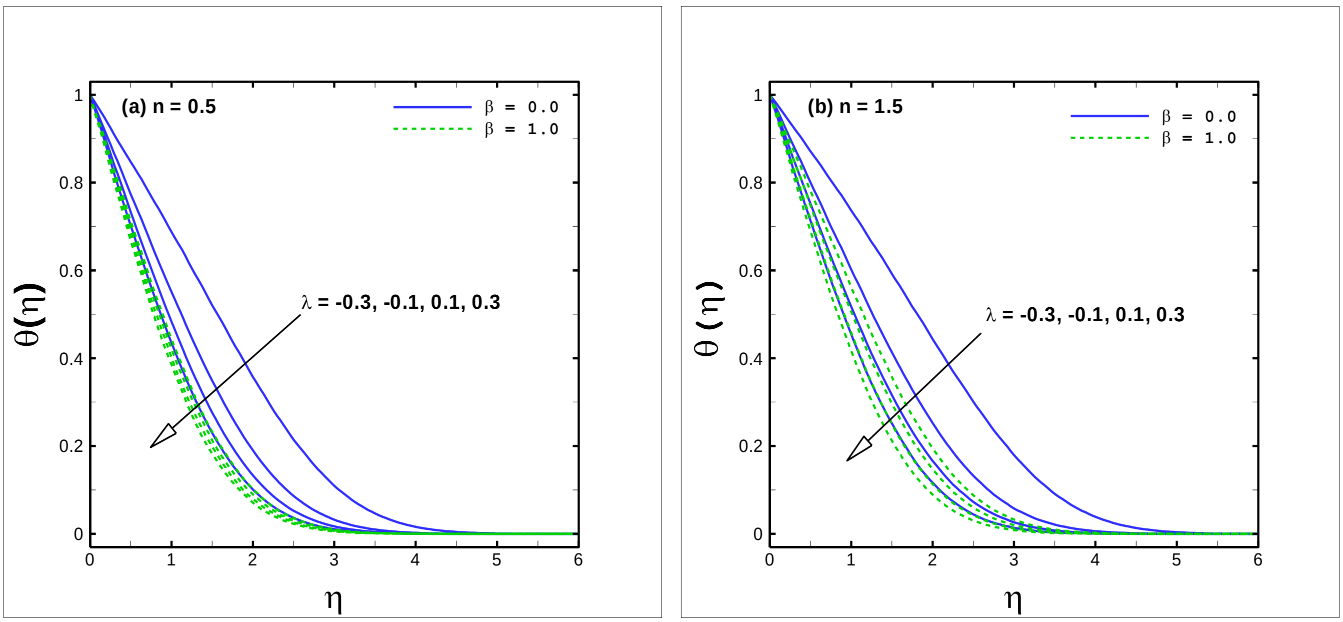

Figure 6: Temperature profiles $\theta(\eta)$ for different λ with $We = 3.0$ and $Pr = 1.0$.

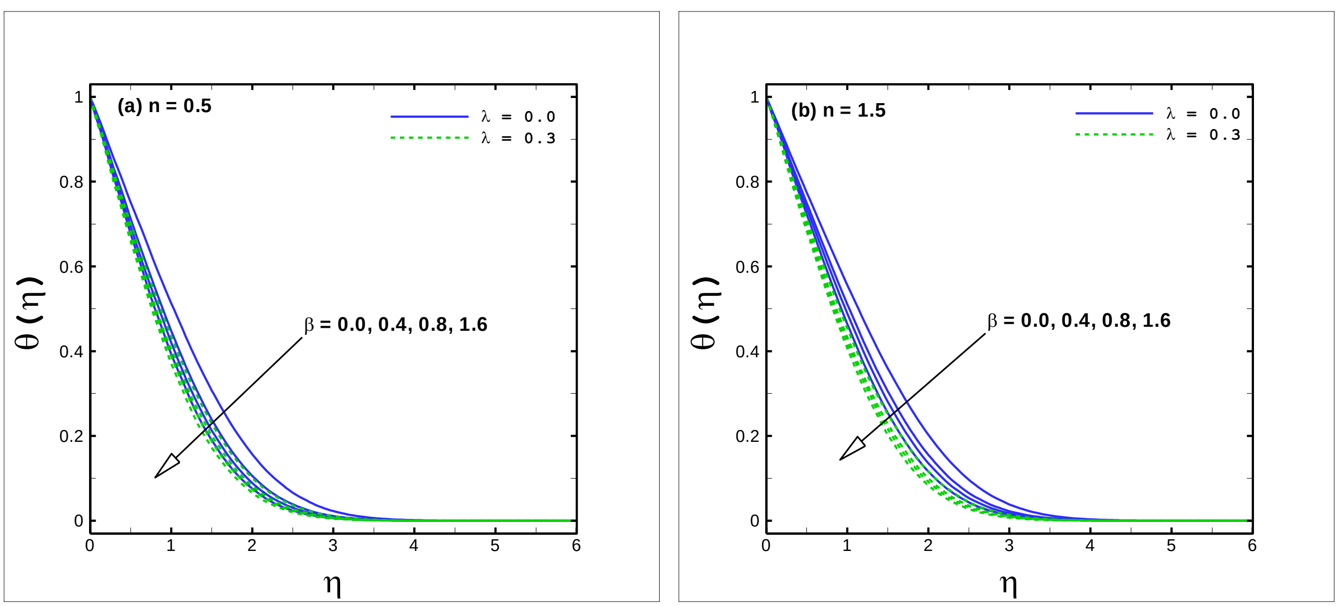

Figure 7: Temperature profiles $\theta(\eta)$ for different β with $We = 3.0$ and $Pr = 1.0$.

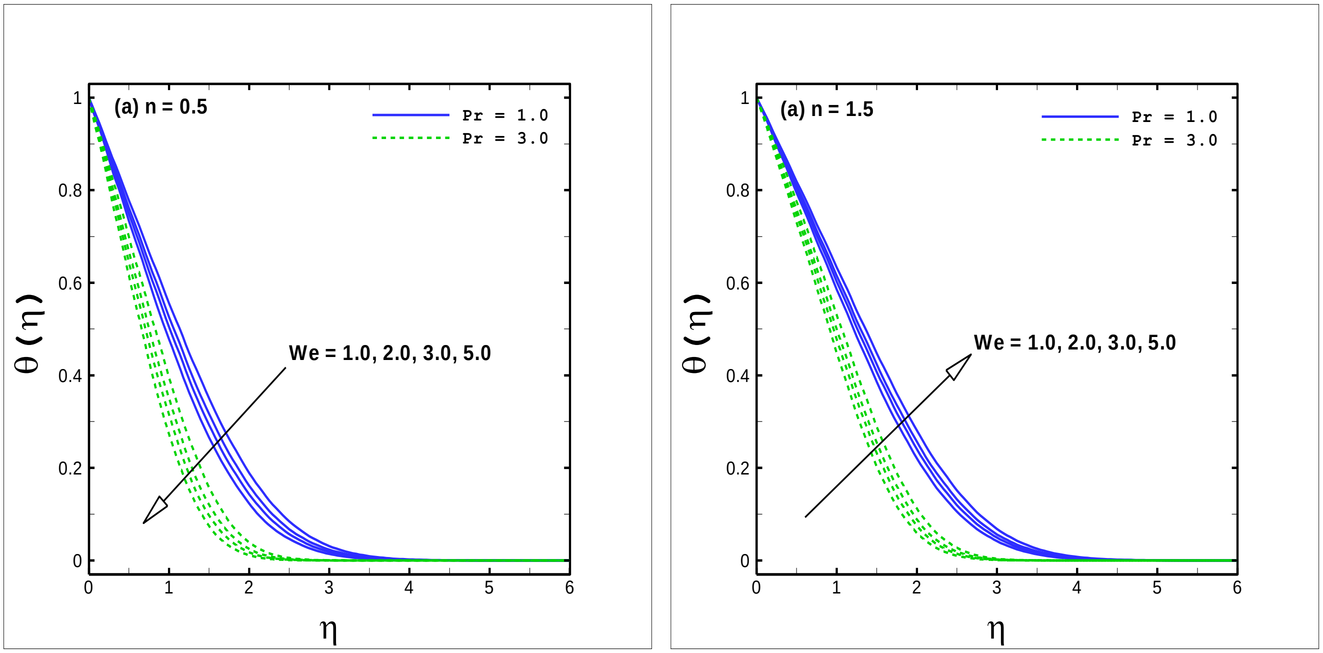

Figure 8: Temperature profiles $\theta(\eta)$ for different We with $\beta = 0.4$ and $\lambda = -0.3$.

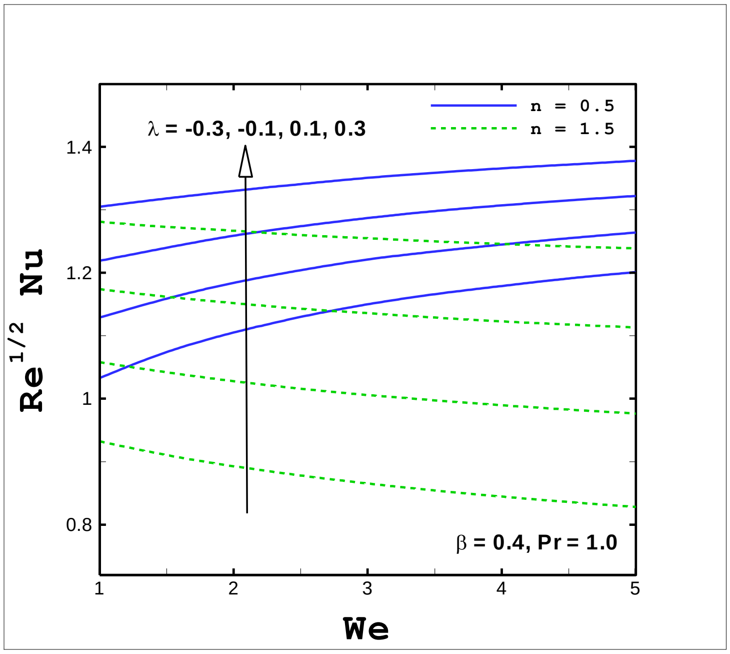

Figure 9: Variation of the Nusselt number $Re^{-1/2}Nu$ with We for different λ.

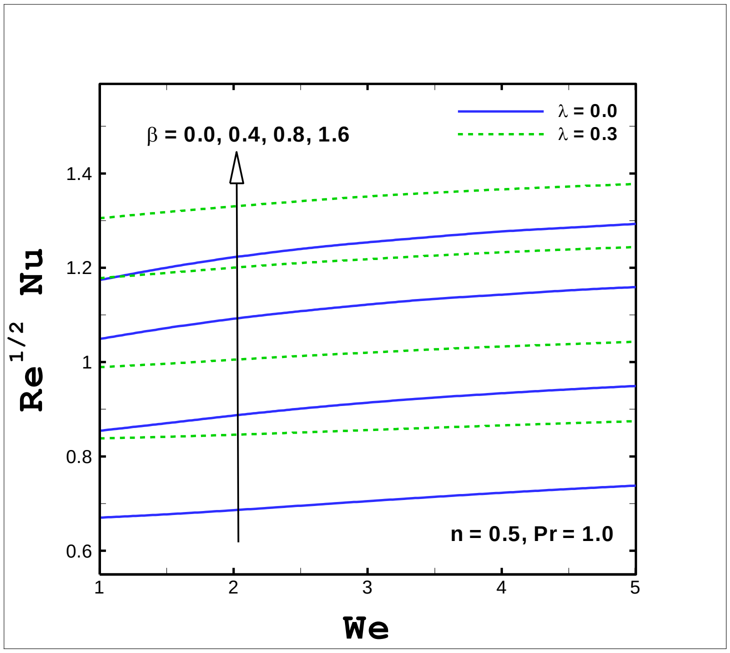

Figure 10: Variation of the local Nusselt number $\mathrm{Re}^{-1/2}\, Nu$ with We for different β.

Concluding notes

This review manages to focus on the momentum and thermal boundary layer characteristics of the Carreau constitutive model past a static/moving wedge. The local similarity variables have been exhibited which change the basic governing differential equations into a set of ordinary differential equations. We facilitate finding the solutions of these conventional differential equations with a numerical strategy known as shooting technique. Results for the skin friction coefficient, local Nusselt number, velocity and temperature profiles were accounted for. From the outcomes it was noticed that the findings of this study were in great concurrence with already distributed works for some specific cases. The guideline consequences of the paper can be compacted as takes after:

- Reduction in the momentum and additionally the thermal boundary layer thicknesses were seen with the development of the wedge angle parameter.
- As the velocity ratio parameter turned out to be huge the velocity of the fluid was expanded, however an inverse conduct was seen in the fluid temperature.
- The local skin friction was larger for the moving wedge with increasing value of wedge angle parameter.
- We got the greatest estimation of skin friction on account of flow close to the stagnation point $(\beta = 1.0)$ for the static wedge.
- The local Nusselt number and local skin friction have displayed opposite behaviors with increasing values of the velocity ratio parameter.
- It was seen that the impact of expanding the Weissenberg number was to upgrade the local Nusselt number.

Nomenclature			
(x, y)	Space coordinates	ψ	Stream function
(u, v)	Velocity components	η	Similarity variable
τ	Stress tensor	f	Dimensionless stream function
μ	Generalized Newtonian viscosity	$f^{/}$	Dimensionless stream function
μ_0	Zero shear viscosity	θ	Dimensionless temperature
μ_∞	Infinite shear viscosity	We	Local Weissenberg number
n	Power law index	β	Wedge angle parameter
Γ	Relaxation time	λ	Velocity ratio parameter
$\dot{\gamma}$	Magnitude of deformation rate	Pr	Prandtl number
u_w	Stretching velocity	c_p	Specific heat
u_e	Free stream velocity	k	Thermal conductivity
b, m, c	Constants	Ω	Wedge angle
T	Fluid temperature	C_f	Skin friction
T_w	Surface temperature	Nu	Nusselt number
T_∞	Free stream temperature	τ_w	Surface shear stress
ν	Kinematic velocity	q_w	Surface heat flux
α	Thermal diffusivity	R_e	Local Reynold number

References

[1] Falkner, V. M., Skan, S. W., Some approximate solutions of the boundary-layer equations, *Philos. Mag.*, *12* (1931), pp. 865-896 .

[2] Hartree, D. H., On an equation occurring in Falkner and Skan's approximate treatment of the equations of the boundary layer, *Proc. Camb. Philos. Soc.*, *33* (1937), pp. 223-239 .

[3] Riley, N., Weidman, P. D., Multiple solutions of the Falkner-Skan equation for flow past a stretching boundary, *SIAM J. Apple. Math.*, *49* (1989), pp. 1350-1358 .

[4] Watanabe, T., Thermal boundary layer over a wedge with uniform suction or injection in force flow, *Acta Mech.*, *83* (1990), pp. 119-126.

[5] Ishak, A., Nazar, R., Pop, I., MHD boundary layer flow past a moving wedge, *Magnetohydrodynamics*, *45* (2009), pp. 3-10 .

[6] Schlichting, H., Gersten, K., Boundary Layer Theory, Springer, Berlin, 2000.

[7] Hayat, T., Khan, M, I., Farooq, M., Alsaedi, A., Waqas, M., Yasmeen, T., Impact of Cattaneo-Christov heat flux model in flow of variable thermal conductivity fluid flow over a variable thicked surface, *Int. J. Heat Mass transf.*, 99 (2016), pp. 702-710.

[8] Hayat, T., Khan, M, I., Farooq, Yasmeen, T., Alsaedi, A., Stagnation point flow with Cattaneo-Christov heat flux and homogeneous-heterogeneous reactions, *J. Mol. Liq.*, 220 (2016), pp. $49 - 55$.

[9] Hayat, T., Imtiaz, M., Alsaedi, A., Unsteady flow of nanofluid with double stratification and magnetohydrodynamics, *Int. J. Heat Mass transf.*, 92 (2016) pp. 100-109.

[10] Hayat, T., Shafiq, A., Imtiaz, M., Alsaedi, A., Impact of melting phenomenon in the Falkner-Skan wedge flow of second grade nanofluid: A revised model, *J. Mol. Liq.*, 215 (2016), pp. 664-670.

[11] Bird, R. B., Curtiss, C. F., Armstrong, R. C., Hassager, O., Dynamics of Polymeric Liquids, John Wiley and Sons Inc., New York, USA, 1987.
[12] Slattery, J. C., Advanced Transport Phenomena, Cambridge University Press, Cambridge, USA, (1999).
[13] Carreau, P. J., Rheological equations from molecular network theories, *Trans. Soc. Rheol., 16* (1972), pp. 99-127 .
[14] Chapkove, A. D., Bair, S., Cann, P., Lubrecht, A. A., Film thickness in point contacts under generalized Newtonian EHL conditions: numerical and experimental analysis, *Tribol. Int.,* 40 (2007), pp. 1474 − 1478.
[15] Jang, J. Y., Khonsari, M, M., Bair, S., On the elastohydrodynamic analysis of shear-thinning fluids, Proc. R. Soc. A., 463 (2007), pp. 3271 − 3290.
[16] Khellaf, K., Lauriat, G., Numerical study of heat transfer in a non-Newtonian Carreau-fluid between rotating concentric vertical cylinders, *J. Non-Newtonian Fluid Mech., 89* (2000), pp. 45-61.
[17] Olajuwon, B. K., Convection heat and mass transfer in a hydromagnetic Carreau fluid past a vertical porous plate in presence of thermal radiation and thermal diffusion, *Thermal Sci.,* 15 (2011), pp. 241-252.
[18] Martins, R. R., Silveira, F. S., Martins-Costa, M. L., Frey, S., Numerical investigation of Inertia and shear-thinning effects on axisymmetric flows of Carreau fluids by a Galerkin least-squares method, *Latin American Appl. Research, 38* (2008), pp. 321-328 .
[19] Khan. M., Hashim, Boundary layer flow and heat transfer to Carreau fluid over a nonlinear stretching sheet, *AIP Advances 5,* 107203 (2015), doi: 10.1063/1.4932627.
[20] Rajagopal, K. R., Gupta, A. S., Nath, T. Y., A note on the Falkner-Skan flows of a non-Newtonian fluid, *Int. J. Nonlinear Mech., 18* (1983), pp. 313-320.
[21] Kuo, B. L., Application of the differential transformation method to the solutions of Falkner-Skan wedge flow, *Acta Mech., 164* (2003), pp. 161-174 .
[22] Ishak, A., Nazar, R., Pop, I., Moving wedge and flat plate in a micropolar fluid, *Int. J. Eng. Sci., 44* (2006), pp. 1225-1236.
[23] White, F. M., Viscous Fluid Flow, McGraw-Hill, New York, USA, 1991.

Paper submitted: January 14, 2016
Paper revised: June 23, 2016
Paper accepted: June 27, 2016